Néel transition and sublattice magnetization of pure and doped La_2CuO_4

B. Keimer
Center for Materials Science and Engineering, Massachusetts Institute of Technology, Cambridge, Massachusetts 02139

A. Aharony
Center for Materials Science and Engineering, Massachusetts Institute of Technology, Cambridge, Massachusetts 02139 and School of Physics and Astronomy, Tel Aviv University, Tel Aviv 69978, Israel

A. Auerbach
Department of Physics, Boston University, Boston, Massachusetts 02215

R. J. Birgeneau and A. Cassanho
Center for Materials Science and Engineering, Massachusetts Institute of Technology, Cambridge, Massachusetts 02139

Y. Endoh
Department of Physics, Tohoku University, Sendai 980, Japan

R. W. Erwin
National Institute of Standards and Technology, Gaithersburg, Maryland 20899

M. A. Kastner
Center for Materials Science and Engineering, Massachusetts Institute of Technology, Cambridge, Massachusetts 02139

G. Shirane
Brookhaven National Laboratory, Upton, New York 11973
(Received 12 August 1991)

We have measured the sublattice magnetization of stoichiometric La_2CuO_4 ($T_N=325$ K) and $La_2Cu_{0.95}Zn_{0.05}O_4$ ($T_N=157$ K). We discuss the data for La_2CuO_4 and other lamellar copper oxides in terms of the quantum Heisenberg model including weak XY anisotropy and interlayer coupling. Spin-wave theory and a generalized Schwinger-boson mean-field theory are used to predict the ordered moment as a function of temperature without adjustable parameters. We also discuss the influence of different dopants on the Néel temperature and sublattice magnetization.

I. INTRODUCTION

The discovery of high-temperature superconductivity in CuO_2-based materials has generated a remarkable wave of progress in research on two-dimensional (2D) quantum magnetism. Stimulated by quasielastic neutron scattering experiments on La_2CuO_4,[1] the dynamical structure factor of the 2D Heisenberg antiferromagnet was calculated[2] by mapping the quantum Heisenberg Hamiltonian onto a $(2+1)$-dimensional nonlinear σ model. These predictions were later confirmed in great detail by inelastic neutron scattering.[3] The recently developed Schwinger-boson mean-field theory (SBMFT)[4] allows a unified treatment of quantum magnets in the ordered and in the rotationally symmetric phases. For the spin-$\frac{1}{2}$ Heisenberg model, this approach agrees to one-loop order with spin-wave theory at $T=0$ and with the nonlinear σ model predictions for $T>0$.

In this paper we report neutron scattering measurements of the sublattice magnetization of carrier-free La_2CuO_4 ($T_N=325$ K) and $La_2Cu_{0.95}Zn_{0.05}O_4$ ($T_N=157$ K). Spin-wave theory is well established as a tool to describe the sublattice magnetization of antiferromagnets and has been used successfully in the past to analyze the temperature dependence of the ordered moments of layered antiferromagnets.[5] Several studies have addressed this problem in the context of the copper oxide materials.[6–9] However, a close examination reveals some deficiencies in the work reported to date. Most authors[6–8] ignore the spin anisotropy of XY symmetry and focus exclusively on the interlayer coupling as a perturbation to the 2D Heisenberg Hamiltonian. Based on independent measurements of the interaction parameters we will show in this paper that an analysis that ignores the XY anisotropy is *incomplete*. A recent study[9] that also considers the XY anisotropy overestimates the anisotropy gaps in the spin-wave spectrum by almost 1 order of magnitude. After a brief review of the experimental situation we analyze our data without adjustable parameters, using only the correct experimentally determined parameters. We also discuss precursor materials of different high-temperature superconductors in this

framework.

Spin-wave theory describes the low-temperature correction to the ordered moment, but not the behavior near and above the Néel temperature. In order to describe the behavior at higher temperatures we use a generalized version of the Schwinger-boson mean-field theory which includes both perturbations self-consistently. We find good agreement between our theory and the data up to $T \sim 0.8 T_N$. At this level the Schwinger-boson mean-field theory may be regarded as a self-consistent spin-wave theory so that spin-wave interaction effects are included. Above $0.8 T_N$ critical fluctuations near the phase transition come into play. We obtain an analytic formula for the Néel temperature that clarifies the basis for the similarity of T_N in materials with vastly different interlayer couplings. We also compare the effect on T_N of static vacancies, introduced into the CuO_2 sheets in the form of nonmagnetic Zn^{2+} ions, with the effect of mobile vacancies in the $Pr_{2-x}Ce_xCuO_4$ system,[10] and are thus able to separate the relative roles of itineracy and dilution in the suppression of T_N. To our surprise, and in contrast to previously reported work on powder samples,[11] we find that T_N is suppressed at the same rate in both systems. We conclude that in electron-doped materials percolative effects are dominant in the destruction of the Néel state, whereas in the hole-doped materials frustrating interactions lead to a much more rapid suppression of T_N.

II. EXPERIMENTAL RESULTS

Large single crystals ($\sim 0.5-1$ cm^3) were grown by the top-seeded solution method as described in detail in previous publications.[12] The sample compositions were determined by electron probe microanalysis. As-grown crystals of the La_2CuO_4 structure are known to contain a small amount of excess oxygen in interstitial sites. These defects introduce carriers into the CuO_2 planes and depress the ordering temperature. We annealed an as-grown La_2CuO_4 crystal for $\frac{1}{2}$ h at 900 °C in vacuum ($\sim 10^{-6}$ Torr). After this procedure, our crystal showed a Néel transition at 325 K, identical to the highest T_N yet achieved for La_2CuO_4 ceramics. Transport measurements show that as T_N increases the resistivity also increases progressively.[13] We therefore assume that all shallow acceptors have been removed from the sample; although we refer to this sample as stoichiometric, it is only important that it contain no excess holes. This technique was also applied to some Zn-doped samples to be discussed below.

The neutron scattering experiments were carried out at the National Institute of Standards and Technology (NIST) research reactor utilizing the *BT*-4 and *BT*-9 triple-axis spectrometers. The incident neutron energies were either 14.7 or 30.5 meV. A pyrolytic graphite filter was inserted into the incident neutron beam to minimize contamination from higher-order reflections.

The magnetic structure of pure La_2CuO_4 is such that the scattering intensity at the (1 0 0) position in reciprocal space is directly proportional to the square of the sublattice magnetization (*Cmca* notation will be used throughout this paper). Above T_N only a small, temperature-independent peak due to double-scattering processes is observed at this position, and this can be readily subtracted from the low-temperature data. The integrated intensities of the (1 0 0) peak are shown in Fig. 1 for our stoichiometric La_2CuO_4 sample and in Fig. 2 for the doped samples.

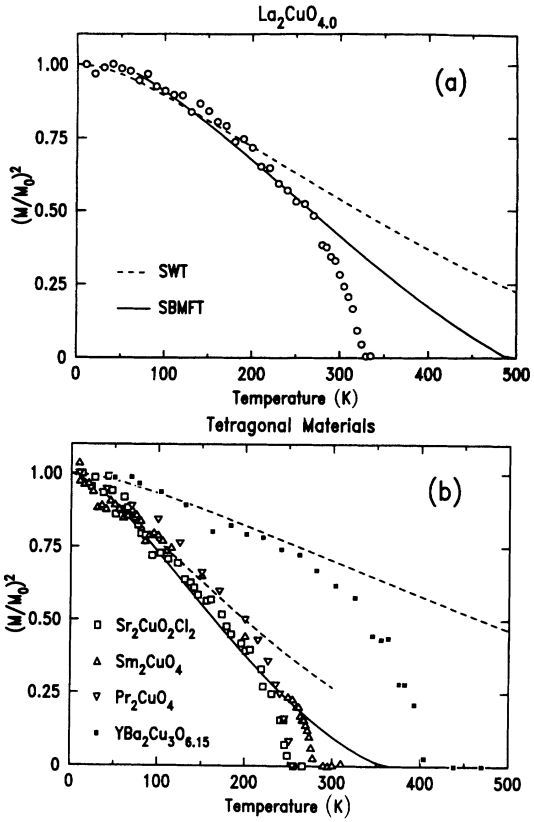

FIG. 1. Sublattice magnetization for orthorhombic (a) and tetragonal (b) materials. The broken lines are the predictions of harmonic spin-wave theory. The solid lines represent the predictions of Schwinger-boson mean-field theory. The data for $YBa_2Cu_3O_{6.15}$ are from Ref. 15.

III. THEORY

The spin Hamiltonian appropriate for a weakly anisotropic, nearly 2D Heisenberg tetragonal antiferromagnet is

$$H = J \left[\sum_{i,\delta_\parallel} \mathbf{S}_i \cdot \mathbf{S}_{i+\delta_\parallel} + \alpha_{xy} \sum_{i,\delta_\parallel} S_i^z S_{i+\delta_\parallel}^z + \sum_{i,\delta_{\perp j}} \alpha_{\perp j} \mathbf{S}_i \cdot \mathbf{S}_{i+\delta_{\perp j}} \right], \quad (1)$$

where α_{xy}, $\alpha_\perp \ll 1$ and $\delta_\parallel, \delta_{\perp j}$ are the nearest-neighbor spacings for the principal directions in-plane and out-of-plane, respectively. In a simple-tetragonal geometry, the energy spectrum in the harmonic approximation is given by

$$\hbar\omega_{qj}=2.32J\sqrt{(1+\tfrac{1}{2}\alpha_\perp\pm\tfrac{1}{2}\alpha_{xy}\gamma_\parallel)^2-(\gamma_\parallel+\tfrac{1}{2}\alpha_\perp\gamma_\perp-\tfrac{1}{2}\alpha_{xy}\gamma_\parallel)^2}\ , \tag{2}$$

where $\gamma_\parallel=[\cos(q_x a)+\cos(q_y a)]/2$, $\gamma_\perp=\cos(q_z c)/2$. The + sign ($j=1$) corresponds to an in-plane polarized mode, the − sign ($j=2$) to an out-of-plane polarized mode. All of the materials to be discussed here depart from this simple-tetragonal structure. We discuss these deviations briefly.

In the temperature range in which magnetic long-range order exists, pure and doped La_2CuO_4 are actually body-centered orthorhombic, so that $\gamma_\parallel$ has a more complicated structure that involves the near-cancellation of two out-of-plane exchange terms. The orthorhombic distortion also manifests itself in an antisymmetric exchange term that introduces a small gap in the in-plane polarized spin-wave mode.[14] In our calculations, corrections due to the orthorhombicity were found to be less than the statistical error in our data, and we will ignore them henceforth for simplicity. Other materials to be discussed later in this paper including $Sr_2CuO_2Cl_2$,[15] Pr_2CuO_4,[16] and Sm_2CuO_4,[17] are actually body-centered tetragonal. The exchange coupling between nearest-neighbor (NN) planes is fully frustrated in this structure. The net 3D coupling responsible for the transition to 3D long-range order must therefore be due to dipolar interactions between NN planes or exchange interactions between NNN planes, possibly enhanced by different mechanisms, such as polarization of any rare-earth moments present in the structure. Again, we do not expect details of the dispersion relation perpendicular to the planes to be important, and we assume a simple-tetragonal structure in our calculations.

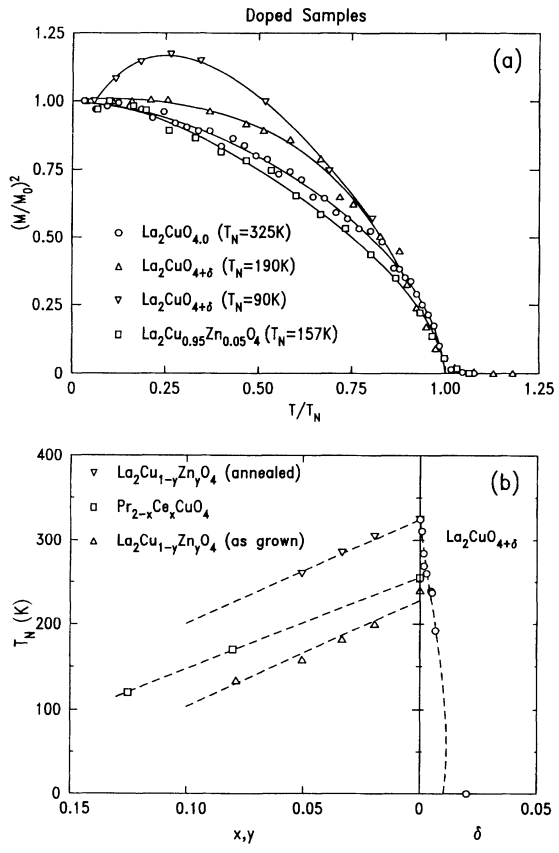

FIG. 2. (a) Order-parameter curves in reduced units for oxygen- and zinc-doped samples. The solid lines are guides to the eye. The data for the oxygen-doped samples are from Ref. 1. (b) Néel temperature as a function of electron and hole concentration. δ was determined by Hall effect measurements (Ref. 27). For the Zn-doped samples, T_N was determined by SQUID magnetometry.

$YBa_2Cu_3O_{6+x}$ does have a simple-tetragonal structure for $x\leq 0.5$. Because of the bilayer structure, however, the spin-wave spectrum is more complicated.[18] It consists of two acoustic branches, split at $\mathbf{q}=0$ by an anistropy gap, and two optical branches, which correspond to antiphase motion of spins within one bilayer. Since the bilayers are very tightly coupled,[18,19] the optical modes are not thermally excited in the temperature range under investigation, and will not contribute to the reduction of the sublattice magnetization. The order-parameter curve is therefore appreciably flatter at low temperatures than in the single-layer materials, as shown in Fig. 1(b).

Most of the parameters entering the spin-wave dispersion relations have been measured experimentally. An extensive discussion can be found in Ref. 16. We briefly summarize this discussion as follows. For La_2CuO_4, $\alpha_\perp=5\times10^{-5}$ is known from magnetoresistance measurements[20] while $J=140$ meV and $\alpha_{xy}=3\times10^{-5}$ have been measured by neutron and light scattering.[14] In the tetragonal one-layer materials various measurements yield $J\approx130$ meV. In Sr_2CuOCl_2 (Ref. 15) $\alpha_{xy}\sim1.5\times10^{-4}$ and we assume that this holds for all of the one-layer tetragonal materials; there is no direct measure of $\alpha_\perp$ but $\alpha_\perp=2\times10^{-8}$ can be calculated for the magnetic dipole interaction between NN layers.[15] For $YBa_2Cu_3O_6$, $J=120$ meV is found by light scattering,[21] $\alpha_{xy}=1.5\times10^{-4}$ and $\alpha_\perp=3\times10^{-5}$ can be deduced from neutron scattering experiments on oxygenated crystals.[18]

In order to encompass the 3D Néel transition in our analysis we have produced a generalization of SBMFT. The ordering is induced by an effective interlayer field and an anisotropy field related to $\alpha_\perp$ and α_{xy}, respectively. This approximation breaks down at temperatures less than the gap temperature, where z-direction spin waves should be properly treated. This theory does not include critical fluctuations near T_N. It does, however, include the rapidly decreasing intralayer correlations which are responsible for the linearly decreasing moment in most of the ordered phase.

A detailed review of the Schwinger boson analysis is given elsewhere.[22] In contrast to Holstein-Primakoff bosons, the spin operators are represented by *two* boson operators per site. The spin-wave spectrum therefore consists of four branches which are degenerate in the un-

perturbed model. The mean-field Hamiltonian for this model can be written as

$$H=\sum_{j=1}^{4}\sum_{\mathbf{q}}\omega_{\mathbf{q}j}(b_{\mathbf{q}j}^{\dagger}b_{\mathbf{q}j}+\tfrac{1}{2})+4Q^2/J-\lambda(2S+1)\ , \tag{3}$$

where Q and λ are the Hubbard-Stratonovich and constraint variational parameters, respectively. The $b_{\mathbf{q}}$ are appropriate linear combinations of boson operators.

The exchange anisotropy and the interlayer exchange split the degeneracy between the four spin-wave modes. We treat the interlayer exchange in a mean-field approximation as an effective staggered field h acting on the planar antiferromagnet. Such an effective staggered field was successfully used in a related mean-field treatment by Thio *et al.*[20] Likewise, we decouple the anisotropy term which results in an effective anisotropy field h_a. In the presence of the fields h and h_a, the mode dispersons become

$$\hbar\omega_{\mathbf{q}j}=C\sqrt{(1+\Delta+4h_a\pm 4h_a+\tfrac{1}{2}h\pm\tfrac{1}{2}h)^2-\gamma_{\parallel}^2}\ , \tag{4}$$

C is weakly temperature and field dependent and can be replaced by its unperturbed value of $2.32J$. $j=1\cdots 4$ correspond to the sign combinations $++$, $-+$, $+-$, $--$. 1,3 (2,4) are the analogues of out-of-plane (in-plane) polarized modes in linear spin-wave theory; 1,2 (3,4) correspond to antiphase (in-phase) motion of NN spins in adjacent layers. Δ is an intrinsic variational gap parameter which in the absence of perturbations reduces to $\Delta_0=\xi_{2D}^{-2}/16$ where ξ_{2D} is the 2D correlation length in units of the lattice constant. Δ, h, and h_a [scaled by J in Eq. (4)] have to be determined self-consistently. At $T=0$, the mean-field parameters acquire the values $\Delta=0$, $h_a=\alpha_{xy}/8$, and $h=\alpha_{\perp}$. Up to corrections of order α_{xy} and $\alpha_{\perp}$ the four Schwinger boson modes in (4) reduce to the spin-wave modes in (2) with $j=1,2$ and $q_{\perp}=0,\pi/c$. The staggered magnetization is given by

$$M(h,h_a,T)=S+\frac{1}{2}-\sum_{j=1}^{2}\sum_{\mathbf{q}}I_{\mathbf{q}j}(h,h_a,T)\ , \tag{5}$$

where we defined $I_{\mathbf{q}j}=(1+\Delta+4h_a\pm 4h_a+\frac{1}{2}h\pm\frac{1}{2}h)[n(\omega_{\mathbf{q}j})+\frac{1}{2}]/\omega_{\mathbf{q}j}$ and $n(\omega)=1/(e^{\hbar\omega/k_BT}-1)$ is the Bose factor. Self-consistency is achieved if h is set to $2\alpha_{\perp}M$ and $h_a=(\alpha_{xy}/2)\sum_{\mathbf{q}}(I_{\mathbf{q}1}+I_{\mathbf{q}3}-I_{\mathbf{q}2}-I_{\mathbf{q}4})$. Finally, the constraint equation, ensuring $2S$ Schwinger bosons at each site, yields $\sum_{j=1}^{4}\sum_{\mathbf{q}}I_{\mathbf{q}j}=2S+1$, which must be obeyed at each temperature. The constraint allows us to reduce the number of low-lying modes from 4 to 2 in Eq. (5). Note that at $T=0$ the lowest mode in Eq. (4) "Bose condenses" and the $\mathbf{q}=0$ fraction of $\sum_{\mathbf{q}}I_{\mathbf{q}4}$ is adjusted to satisfy the constraint.

Figure 1(a) shows a numerical evaluation of Eq. (5) for La_2CuO_4 ($\alpha_{xy}=3\times10^{-5}$, $\alpha_{\perp}=5\times10^{-5}$, $J=140$ meV); Fig. 1(b) shows the results for the tetragonal one-layer material ($\alpha_{xy}=1.5\times10^{-4}$, $\alpha_{\perp}=2\times10^{-8}$, $J=130$ meV). Obviously, the agreement between our prediction and the experimental data is very satisfactory up to about 270 K in La_2CuO_4, and up to about 250 K for Sm_2CuO_4 and $Sr_2CuO_2Cl_2$. These are temperatures where critical fluctuations are expected to become important. We should also note that variations by factors of 2 for either α_{xy} or $\alpha_{\perp}$ have little effect on the theoretical curves.

At low temperatures ($T<2J\sqrt{\alpha_{\perp}}$) the effective-field approximation yields a spurious "gap" in the spin-wave spectrum. We therefore used a standard 3D spin-wave analysis based on the dispersion relations given in Eq. (2). The results are shown in Fig. 1. At elevated temperatures the range of the in-plane correlations is sharply reduced and harmonic spin-wave theory fails. This is in general agreement with neutron scattering measurements on La_2CuO_4 which indicate systematic departures from spin-wave theory as the temperature is raised well above $T=0$.[3] We emphasize that spin-wave theory and the Schwinger Boson mean-field theory cover complementary temperature regimes. While the first strictly holds in the regime of large staggered magnetization, the latter is a self-consistent mean-field theory, which can be applied at higher temperatures $2J\sqrt{\alpha_{\perp}}<T<T_N$, where the ordered moments are considerably reduced.

It should also be noted that both the Schwinger boson and spin-wave theories explicitly give $2M_0\sim0.6$ and the good agreement between theory and experiment evident in Fig. 1 rests on this prediction. This in turn necessitates that the smaller values for M_0 typically reported in the literature[1,3,15] must reflect the effects of covalency and, in certain cases, inadvertent dopants.

It has recently been pointed out[16] that the interlayer coupling in the tetragonal materials is much too small to account for an ordering temperature of ~250 K. In order to explain the close similarity of the Néel temperatures of La_2CuO_4 ($\alpha_{\perp}=5\times10^{-5}$) and $Sr_2CuO_2Cl_2$ ($\alpha_{\perp}\approx10^{-8}$), the authors of Ref. 16 suggested that the XY anisotropy, which is similar in all lamellar copper oxides, is chiefly responsible for the magnitude of the ordering temperature. Our analysis in the preceding paragraphs lends strong support to this picture.

The Schwinger boson model offers a straightforward way to explore these ideas in a quantitative fashion. Our numerical results are well described by the equation

$$\frac{T_N}{2J}\approx\frac{M_0\pi}{\ln\{4\alpha_{\mathrm{eff}}/[M_0\pi^2\ln(4\alpha_{\mathrm{eff}}/\pi)]\}} \tag{6}$$

with $\alpha_{\mathrm{eff}}=z_{\parallel}\alpha_{xy}+z_{\perp}\alpha_{\perp}$ with $z_{\parallel}=4$ and $z_{\perp}=2$ the in- and out-of-plane coordination numbers, respectively. $2M_0\approx0.6$ is the $T=0$ sublattice magnetization. Equation (6) is derived by solving the SBMFT equations in two limiting cases: $\alpha_{xy}\ll\alpha_{\perp}$, and $\alpha_{xy}\gg\alpha_{\perp}$. The full derivation is deferred to a planned future publication.[22]

The interpretation of Eq. (6) requires some discussion. In the limit $\alpha_{xy}\ll\alpha_{\perp}$ the correlation length crosses over from the behavior of the 2D Heisenberg model,[2] $\xi_{2D}/a\sim e^{2\pi\rho_s/T}$ to that characteristic of the 3D Heisenberg model at a temperature given by $(\xi_{2D}/a)^2\alpha_{\perp}\sim1$. In this limit, Eq. (6) is analogous to similar formulas given in previous studies.[6–8] However, this limit does not actually apply to the layered copper oxide materials. As we have seen above, in La_2CuO_4 $\alpha_{xy}\sim\alpha_{\perp}$ while in the tetragonal single-layer materials $\alpha_{\perp}\ll\alpha_{xy}$. The interpretation of Eq. (6) for $\alpha_{xy}\sim\alpha_{\perp}$ is straightforward. The behavior

for $\alpha_\perp \ll \alpha_{xy}$ is more subtle.

In a theory which went beyond the mean-field approximation one would obtain a crossover to Kosterlitz-Thouless behavior[23] when $(\xi_{2D}/a)^2\alpha_{xy} \sim 1$. Because of the interlayer coupling the Kosterlitz-Thouless transition would be preempted by a 3D XY transition.[16] In spite of the mean-field nature of the Schwinger boson model, analogous behavior is found. Specifically this model gives in the xy regime ξ_{2D} $(XY) \sim \xi_{2D}^2$ (Heisenberg). Thus, the interlayer coupling enters as $\alpha_\perp^{1/2}$ rather than as $\alpha_\perp$ making the *effective* interlayer coupling in the tetragonal materials comparable to that in La_2CuO_4. Thus even for $\alpha_\perp \ll \alpha_{xy}$ the Néel transition temperature is controlled by α_{xy} as predicted by Eq. (6). Of course for $\alpha_\perp^{1/2} \ll \alpha_{xy}$ Eq. (6) no longer holds and a proper Kosterlitz-Thouless-type theory[23] is required.

The absolute magnitudes of the ordering temperatures are overestimated for two reasons. First, the Schwinger boson analysis is known to overestimate the magnetic correlation length ξ_{2D}.[4] Second, our model does not include critical fluctuations. Taking these into account would further reduce the expected value of T_N. In spite of its deficiencies we believe that Eq. (6) provides an adequate description of the relative influence of the perturbative terms on the Néel temperature.

IV. DOPED MATERIALS

Having obtained a good understanding of the pure materials we now turn to the effects of both electrons and holes on the Néel temperature and the shape of the order-parameter curve. Order-parameter curves for $La_2CuO_{4+\delta}$ with increasing δ are shown in Fig. 2(a). Upon oxygenation of La_2CuO_4 the order-parameter curve first flattens and ultimately exhibits reentrant behavior at low temperatures. This change in shape reflects the influence of the "central peak" spin excitations induced by the holes which become prominent at low temperatures.[1,14] By contrast, substitution of Zn^{2+} for Cu^{2+} introduces no such reentrancy. Notice that if the temperature is scaled by T_N, as in Fig. 2, the order-parameter curve for $La_2Cu_{0.95}Zn_{0.05}O_4$ stays very close to the one for pure La_2CuO_4, although the Néel temperatures differ by a factor of more than 2. This is due to the fact that both T_N and the thermal reduction of the sublattice magnetization depend logarithmically on $\alpha_\perp$ and α_{xy} in closely related forms.

The substitution of Zn^{2+} for Cu^{2+} creates an additional electron, but Zn doping does not affect the conductivity, showing that, as expected, the electrons are tightly bound to the Zn impurity. It is very surprising, however, as shown in Fig. 2(b), that it does not seem to matter whether the electrons are localized in this way or itinerant: Doping with Ce in $Pr_{2-x}Ce_xCuO_4$ has the same effect on T_N as doping with Zn in $La_2Cu_{1-y}Zn_yO_4$, although the former samples are quite metallic[24] for $x \gtrsim 0.1$.

While there is little difference between the effect on T_N of localized and itinerant electrons, there is a marked difference between the effect of electrons and holes. Whereas a straight-line extrapolation of the data in Fig. 2 for annealed $La_2Cu_{1-y}Zn_yO_4$ gives $T_N = 0$ at $y \sim 0.26$, there is no long-range order in $La_{2-x}Sr_xCuO_4$ for $x \geq 0.02$. The suppression of T_N with electron doping may be consistent with percolation if reduction of J, $\alpha_\perp$, and α_{xy} by doping are accounted for. ($x_c = 0.41$ is the nearest-neighbor percolation threshold for the 2D square lattice.) Frustration, which one might *a priori* expect for a mobile electron localized around a plaquette of the 2D square lattice, does not seem to play a major role in the electron-doped materials. However, the reentrant behavior as well as many simulations[25] suggest that frustration, presumably in the sense of Aharony *et al.*,[26] is the primary cause of the rapid destruction of Néel order in the hole-doped materials. Finally we note that the differences in the Néel temperatures between the as-grown and annealed $La_2Cu_{1-y}Zn_yO_4$ samples are independent of y suggesting that the effects of localized holes on the oxygen sites and electrons on the Cu sites are additive. All of the above results are very difficult to rationalize based on simplified models such as the t-J model for the CuO_2 planes.

ACKNOWLEDGMENTS

Research at MIT was supported by the National Science Foundation under Grants No. DMR 90-22933 and DMR 90-07825. Work at Brookhaven was carried out under Contract No. DE-AC02-76CH00016, Division of Materials Science, U.S. Department of Energy. A. Auerbach acknowledges NSF Grant No. DMR-8914045 and the Sloan Foundation for support. Authors at MIT and Tel Aviv University also acknowledge support by the U.S.-Israel Binational Science Foundation (B.S.F.).

[1] Y. Endoh *et al.*, Phys. Rev. B **37**, 7443 (1988).
[2] S. Chakravarty, B. I. Halperin, and D. R. Nelson, Phys. Rev. B **39**, 2344 (1989); S. Tyc, B. I. Halperin, and S. Chakravarty, Phys. Rev. Lett. **62**, 835 (1989).
[3] K. Yamada *et al.*, Phys. Rev. B **40**, 4557 (1989).
[4] D. P. Arovas and A. Auerbach, Phys. Rev. B **38**, 316 (1988); A. Auerbach and D. P. Arovas, Phys. Rev. Lett. **61**, 617 (1988).
[5] H. W. de Wijn *et al.*, Phys. Rev. Lett. **24**, 832 (1970).
[6] W. Xue *et al.*, Phys. Rev. B **38**, 6868 (1988).
[7] A Singh *et al.*, Phys. Rev. Lett. **64**, 2571 (1990); **67**, 1939 (1991).
[8] C. M. Soukoulis *et al.*, Phys. Rev. B **44**, 446 (1991).
[9] A. Singh and Z. Tesanovic, Phys. Rev. B **43**, 11 445 (1991).
[10] T. R. Thurston *et al.*, Phys. Rev. Lett. **65**, 263 (1990).
[11] Gang Xiao *et al.*, Phys. Rev. B **42**, 240 (1990).
[12] Y. Hidaka *et al.*, J. Cryst. Growth **85**, 581 (1987).
[13] N. W. Preyer *et al.*, Phys. Rev. B **39**, 11 563 (1989).
[14] C. J. Peters *et al.*, Phys. Rev. B **37**, 9761 (1988).
[15] D. Vaknin *et al.*, Phys. Rev. B **41**, 1926 (1990); Y. Endoh *et al.* (unpublished).
[16] M. Matsuda *et al.*, Phys. Rev. B **42**, 10 098 (1990).
[17] S. Skanthakumar *et al.*, J. Appl. Phys. **69**, 4866 (1991).

[18]J. M. Tranquada *et al.*, Phys. Rev. B **40**, 4503 (1989); J. Rossat-Mignod *et al.*, Physica B **163**, 4 (1989).
[19]H. Kadowaki *et al.*, Phys. Rev. B **37**, 7932 (1988).
[20]T. Thio *et al.*, Phys. Rev. B **38**, 905 (1988); T. Thio *et al.*, **41**, 231 (1990).
[21]K. B. Lyons *et al.*, Phys. Rev. Lett. **60**, 732 (1988).
[22]A. Aharony and A. Auerbach (unpublished).
[23]J. M. Kosterlitz and D. J. Thouless, J. Phys. C **6**, 1181 (1973).
[24]K. Hirochi *et al.*, Physica C **160**, 273 (1989).
[25]I. Morgenstern, Z. Phys. B **80**, 7 (1990).
[26]A. Aharony *et al.*, Phys. Rev. Lett. **60** 1330 (1988).
[27]C. Y. Chen *et al.*, Phys. Rev. B **43**, 392 (1991).